

# Rolling of Plates and Sheets from As-Cast Ti-6Al-4V-0.1B

Raghavan Srinivasan, Mats D. Bennett, Seshacharyulu Tamirisakandala, Daniel B. Miracle, Kuang-O (Oscar) Yu, and Fusheng Sun

(Submitted February 13, 2008; in revised form July 30, 2008)

Trace boron addition (~0.1 wt.%) to conventional titanium alloys reduces the as-cast prior-beta grain size by an order of magnitude to about 200  $\mu\text{m}$ , a grain size typically observed after ingot breakdown. In this study, the feasibility of producing plate and sheet by hot rolling of as-cast Ti-6Al-4V-0.1B (wt.%) was evaluated. Starting from an initial thickness of 25 mm, as-cast Ti-6Al-4V-0.1B was successfully rolled to 2 mm sheet in a multistep rolling process. As-cast Ti-6Al-4V (without boron addition) rolled under similar conditions exhibited severe cracking. Tensile properties of the sheets and plates made from the boron-containing alloy met or exceeded AMS 4911 specifications for Ti-6Al-4V plates and sheets produced by conventional processing route. The process of making plate and sheet stock from cast titanium alloy ingots, without recourse to expensive ingot breakdown, can significantly reduce the number of expensive and time-consuming processing steps for making titanium alloy components, thereby enhancing the affordability and expanding the range of titanium applications.

**Keywords** mechanical testing, rolling, titanium

## 1. Background

As-cast titanium alloy ingots have a very coarse prior- $\beta$  grain size (of the order of a few centimeters) that must be refined to an intermediate grain size of ~200  $\mu\text{m}$  for improved strength, ductility, and hot workability. In current practice, this is accomplished through a series of thermomechanical processes, collectively referred to as ingot breakdown and billet conversion. Initial ingot breakdown is done above the beta transus temperature to enable large deformations and low press forces. Much of the billet conversion is done below the beta transus to avoid the rapid grain growth that occurs above the beta transus. This introduces a narrow process window, which, along with workpiece cooling, requires a substantial degree of iterative processing that is an important contributing factor to the long lead times often needed for titanium products. This extensive thermomechanical processing, along with machining losses between steps to remove the alpha case and surface cracking, adds significantly to the cost of titanium mill products (Fig. 1).

For the most commonly used titanium alloy Ti-6Al-4V (Ref 1),  $\beta$  working is done between 1095 and 1150  $^{\circ}\text{C}$ , which is 100 to 150  $^{\circ}\text{C}$  above the beta transus temperature (995  $^{\circ}\text{C}$ ), while  $\alpha + \beta$  working is performed in the temperature range of

860 to 980  $^{\circ}\text{C}$  to convert the coarse-grained microstructure in the as-cast ingots into a fine-grained, equiaxed structure in mill products (Ref 2, 3). The mill product forms are input stocks for subsequent deformation processing such as forging or sheet rolling.

Recent innovations in two areas, ingot melting and minor changes to alloy composition, permit the elimination of a significant portion of the activities shown in the dashed box in Fig. 1. The new melting techniques include single melt techniques, such as plasma arc melting (PAM), induction skull melting (ISM), and electron beam melting (EBM), which could replace the double or triple vacuum arc remelting (VAR) that is currently used to produce ingots of uniform composition (Ref 1).

Trace additions of boron to several standard titanium alloys, such as commercially pure (CP) titanium, Ti-6Al-4V, and Ti-6Al-2Sn-4Zr-2Mo (compositions throughout this manuscript are given in weight percent), dramatically refine the as-cast grain size (Ref 4). Specifically, boron additions on the order of 500-1000 parts per million by weight (wppm) or 0.05-0.1 wt.%, refine the as-cast grain size by roughly an order of magnitude, to levels that can otherwise be accomplished only after ingot breakdown. Concomitant with the decrease in grain size, enhancements in the strength and stiffness by 5% without any loss in ductility were also observed (Ref 5, 6). Though a growing body of work exists on titanium alloys modified with large boron additions (> 1.5 wt.%) (Ref 7-17), relatively little attention has been given to the deformation processing of alloys with less than 1% boron.

As in other metal industries that rely on inoculants and grain refiners, the casting of reasonably fine-grained billets that can serve as the starting stock of secondary processing may be feasible in the titanium industry. The objective of this paper is, therefore, to explore direct rolling of as-cast Ti-6Al-4V-0.1B to establish if grain refinement via small boron addition can effectively reduce the primary ingot breakdown steps normally required prior to rolling of conventional Ti-6Al-4V ingots. The implication of this work is that there is the potential to significantly modify, reduce, or eliminate the processing steps

Raghavan Srinivasan and Mats D. Bennett, Wright State University, 3640 Col. Glenn Highway, Dayton, OH 45435; Seshacharyulu Tamirisakandala, FMW Composite Systems, Inc. 1200 West Benedum Industrial Drive, Bridgeport, WV 26330; Daniel B. Miracle, Air Force Research Laboratory, Materials and Manufacturing Directorate, Wright-Patterson AFB, Dayton, OH 45433; and Kuang-O (Oscar) Yu and Fusheng Sun, RTI International, 1000 Warren Ave., Niles, OH 44446. Contact e-mail: raghavan.srinivasan@wright.edu.

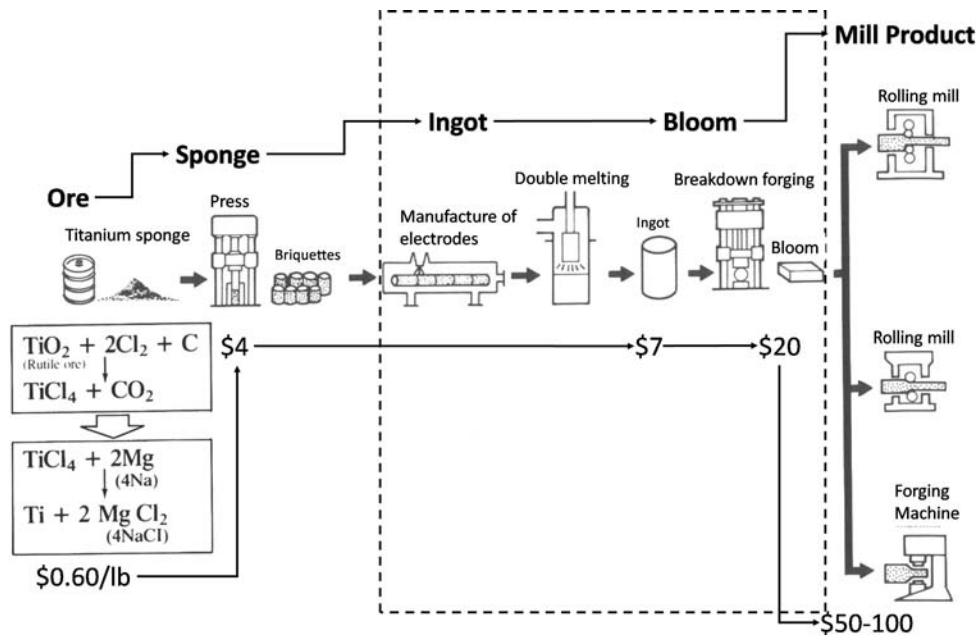


Fig. 1 Change in value of titanium from ore to mill product. Ref: The Economics of Titanium Report, 2004 and (Ref 1)

involved in ingot breakdown and billet conversion currently used in the titanium industry.

## 2. Materials and Experimental Procedures

### 2.1 Materials

Ingots of Ti-6Al-4V and Ti-6Al-4V-0.1B were prepared by plasma arc melting (PAM) at RTI International, Niles, Ohio, and by induction skull melting (ISM) at Flowserve Corp., Dayton, Ohio. These processes can deliver composition uniformity with a single melting, compared to VAR, which, because of the very local melt pool, requires double or triple remelts to ensure a uniform composition. The ISM facility, with a melt capacity of about 35 kg, was the same as that had been used in the earlier studies (Ref 4, 18, 19). The PAM ingots had nominal dimensions of 125 mm (5-in.)  $\phi$  and 900 mm (36-in.) in length, and the ISM ingot was 150 mm (6-in.)  $\phi$ , 200 mm (8-in.) in length (Fig. 2). The compositions are listed in Table 1. The raw materials used in PAM ingots are of aerospace quality while those used in ISM ingots are of commercial quality.

### 2.2 Plate and Sheet Rolling

Starting blanks of 25-mm (1-in.) thickness and 127-mm (5-in.) square were sectioned in the longitudinal direction from each of the PAM ingots. Two blanks, identified as ISM-1-Ti-6Al-4V-0.1B and ISM-2-Ti-6Al-4V-0.1B in Table 2, of 25-mm (1-in.) thickness and 90-mm (3.5-in.) square were sectioned in the transverse direction from the ISM ingot. The ISM billets were heated to 954 °C (1750 °F) in air prior to rolling, and hot rolled per the schedule shown in Table 2 to a thickness of 5.1 or 6.35 mm (0.2 or 0.25 in.) on a 50 Ton laboratory rolling mill at RTI International. The temperature was selected on the basis of a previous study in which samples of as-cast Ti-6Al-4V-0.1B,

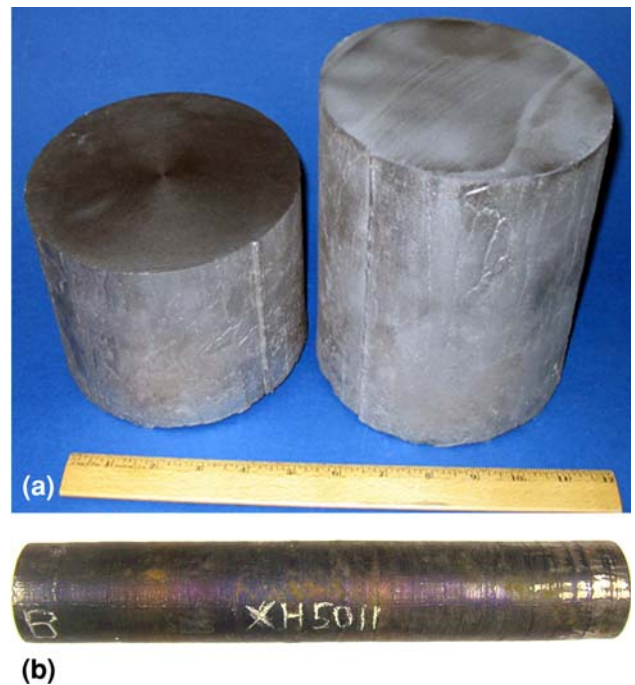


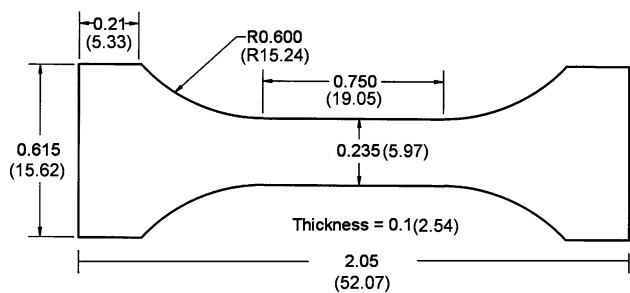
Fig. 2 Ti-6Al-4V + 0.1B ingots produced by (a) ISM and (b) PAM. See Table 1 for dimensions

Table 1 Composition and size of ISM and PAM ingots

ISM 150 mm (6-in.) $\phi$ , 200 mm (8-in.) length	PAM 125 mm (5-in.) $\phi$ , 900 mm (36-in.) length
Ti-6Al-4V	Ti-6Al-4V
Ti-6Al-4V-0.1B	Ti-6Al-4V-0.1B-0.180

**Table 2 Rolling schedule for test materials**

Material	Condition ID	Starting	Roll to	% Red.	Cross-roll to	% Red.
Ingot to plate (nominal dimensions in mm)						
PAM-Ti-6Al-4V-0.1B	PBP	125 × 125 × 25	125 × 250 × 13	50	250 × 250 × 6.35	50
PAM-Ti-6Al-4V	POP	125 × 125 × 25	125 × 200 × 16	38	330 × 200 × 6.35	63
ISM-1-Ti-6Al-4V-0.1B	I1BP	90 × 90 × 25	90 × 180 × 13	50	220 × 180 × 5.1	60
ISM-2-Ti-6Al-4V-0.1B	I2BP	90 × 90 × 25	90 × 140 × 16	35	220 × 140 × 6.35	63
Plate to sheet (nominal dimensions in mm)						
PAM-Ti-6Al-4V-0.1B	PBS	125 × 125 × 6.35	125 × 190 × 4	35	260 × 190 × 2	50
ISM-1-Ti-6Al-4V-0.1B	IBS	111 × 178 × 5.1	260 × 178 × 2.16	59		

**Fig. 3** Tensile test specimen dimensions in inches (mm)

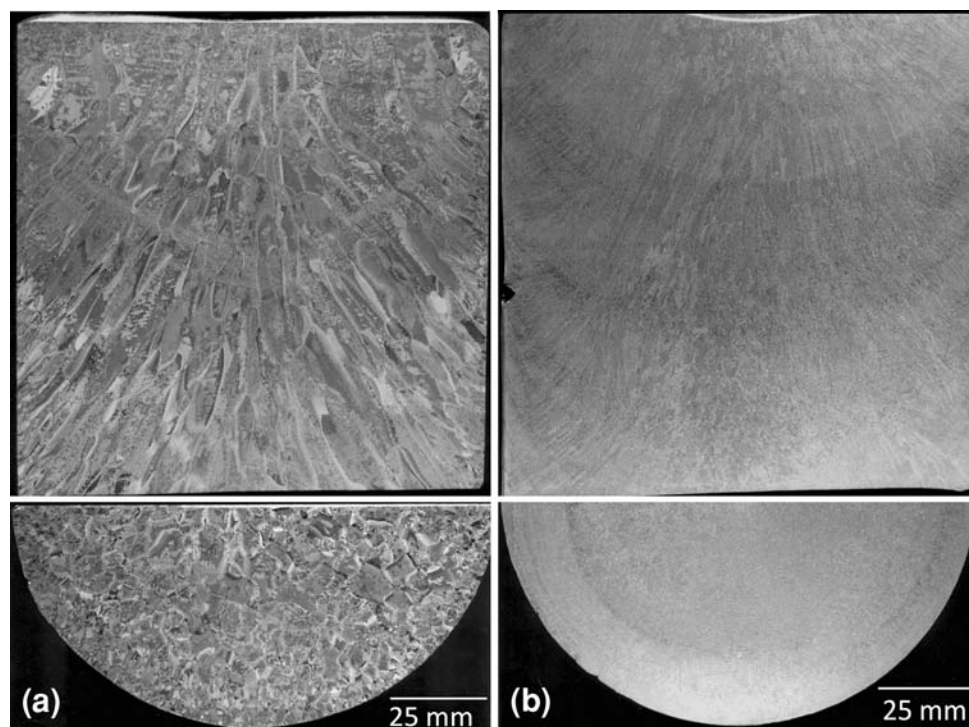
as-cast Ti-6Al-4V, and wrought Ti-6Al-4V were rolled at temperatures in the range of 750 to 950 °C (Ref 18). The roll pass design was selected to mimic the conventional Ti-6Al-4V rolling. Reheating schedule in between rolling passes was left to the discretion of the mill operators. Because excessive chilling was observed when rolling the ISM billets in a prior

study, rolling of the billets of both PAM materials to plates and sheets, as well as the rolling of ISM plates to sheet, was done at 982 °C (1800 °F).

The plate produced by rolling billet ISM-1-Ti-6Al-4V-0.1B was sectioned in half and rolled further to a thickness of 2.16-mm (0.085-in.), as indicated in Table 2. Plates of PAM-Ti-6Al-4V-0.1B and PAM-Ti-6Al-4V materials were sectioned in half, and one half was rolled to sheet. The other half of the PAM plates and the second ISM plate (ISM-2-Ti-6Al-4V-0.1B) were used for tensile samples. The sheets produced from ISM-1-Ti-6Al-4V-0.1B, PAM-Ti-6Al-4V-0.1B, and PAM-Ti-6Al-4V were used for both tensile testing and sheet formability testing.

### 2.3 Heat Treatment of the Rolled Sheets

The sheet samples produced by rolling were given a postdeformation anneal of 15 min at 788 °C (1450 °F) followed by air cooling prior to tensile and formability testing. This was done to produce material with a processing history similar to that typical of Ti-6Al-4V. The plate samples were not subject to heat treatment.

**Fig. 4** Macrographs of PAM cast Ti-6Al-4V ingots showing grain refinement after addition of 0.1 wt.% boron (a) PAM Ti-6Al-4V (b) PAM-Ti-6Al-4V-0.1B

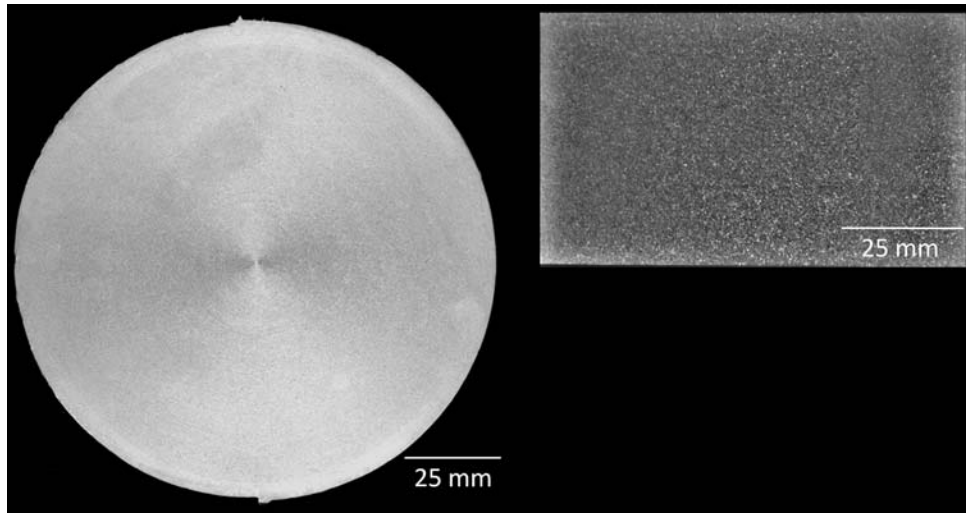


Fig. 5 Macrographs of ISM Ti-6Al-4V + 0.1B ingot

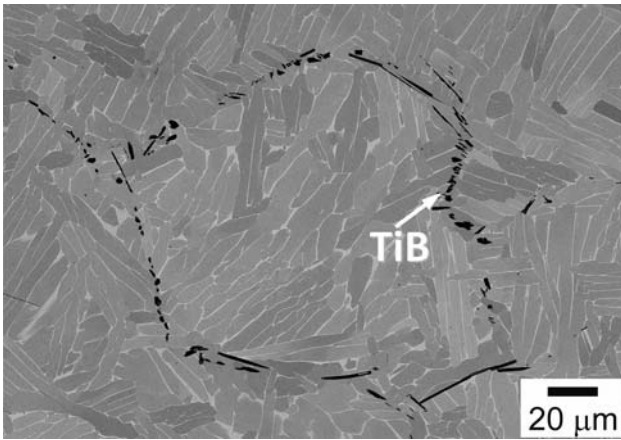


Fig. 6 Typical micrograph of cast ISM Ti-6Al-4V-0.1B

#### 2.4 Tensile and Formability Testing of Plate and Sheet

Tensile samples were sectioned by electric discharge machining (EDM) from the plates and sheets of PAM and ISM Ti-6Al-4V + 0.1B (Fig. 3). The samples were surface

ground prior to testing at room temperature. Tensile tests were performed on a servohydraulic test machine under displacement control at a crosshead speed of  $0.01 \text{ mm s}^{-1}$ , which corresponds to an initial strain rate of  $0.001 \text{ s}^{-1}$  for a 10 mm gage length. Testing was conducted in triplicate and the average values are reported. Tensile elongations were measured with an extensometer attached to the samples, as well as by placing the broken halves together.

The formability of the sheets was evaluated using the double bend test (ASTM E 290). A 25 (1-in.) by 100-mm (4-in.) strip of the material to be tested is bent into a “Z” shape, with the bending axis parallel to the rolling direction. Per AMS 4911J, the bent sample should show no evidence of cracking when examined at 15 to 25 $\times$  magnification. The bend factor (diameter of bend/sheet thickness ratio) for the tests was about 8.

### 3. Results and Discussion

#### 3.1 Starting Microstructures

Macro- and microstructures of the starting materials are shown in Fig. 4-7. Figure 4(a) shows that the PAM Ti-6Al-4V

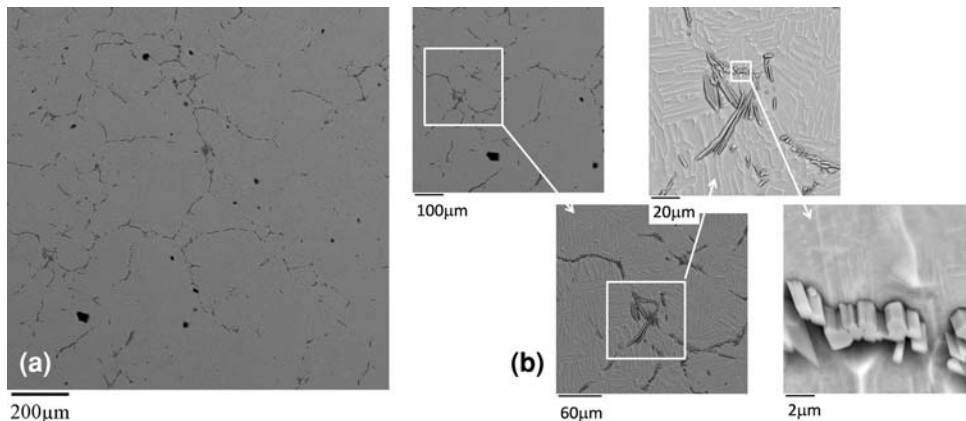
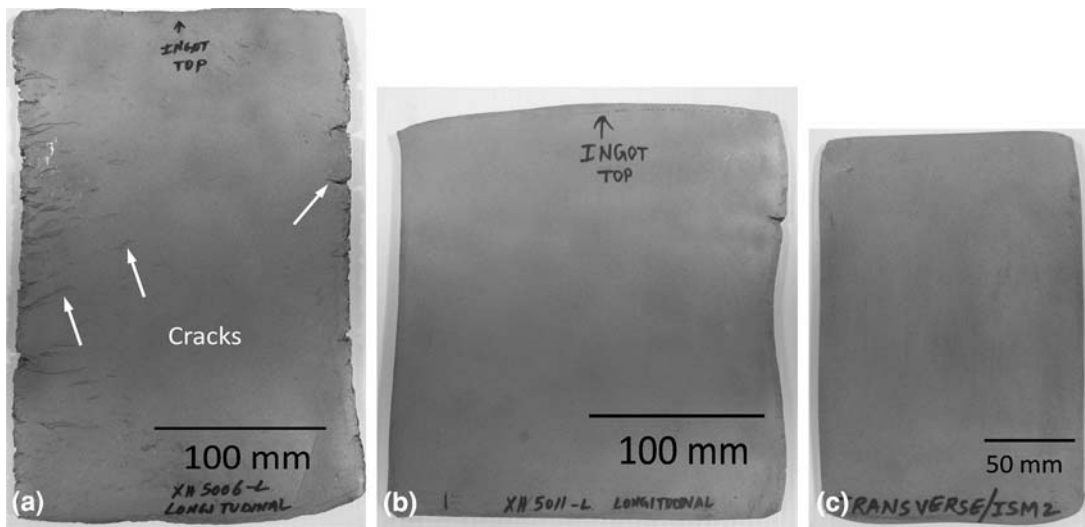


Fig. 7 Deep etched samples of cast ISM Ti-6Al-4V-0.1B showing randomly oriented TiB needles



**Fig. 8** Plates produced from PAM Ti-6Al-4V, PAM Ti-6Al-4V-0.1B, and ISM Ti-6Al-4V-0.1B

ingot has a columnar grain morphology with grains as long as 40 mm and widths up to 10 mm. The addition of 0.1 wt.% B results in a substantial refinement of the as-cast structure seen in the macrograph of PAM Ti-6Al-4V-0.1B shown in Fig. 4(b). The macrograph of the ISM ingot shown in Fig. 5 also reveals a fine as-cast structure. The microstructure of ISM-Ti-6Al-4V-0.1B comprises TiB needles along the prior- $\beta$  grain boundaries, and lamellar  $\alpha + \beta$  colonies in the interior of prior- $\beta$  grains (Fig. 6). Deep etching of the matrix reveals that the needle-shaped TiB particles are randomly oriented on prior- $\beta$  grain boundaries (Fig. 7). The prior-beta grain size in both the boron-containing materials is about 250  $\mu\text{m}$ , and the TiB needles, which make up about 0.5 vol%, are about 1  $\mu\text{m}$  wide and 20 to 25  $\mu\text{m}$  long.

### 3.2 Plate and Sheet Rolling

Figure 8 shows the as-rolled plates of PAM-Ti-6Al-4V and PAM-Ti-6Al-4V-0.1B materials. The coarse columnar grain structure in the PAM-Ti-6Al-4V material required that it be rolled primarily in the longitudinal direction of the ingot, resulting in a rectangular plate, while the PAM-Ti-6Al-4V-0.1B material could be cross-rolled, producing a square plate. Several large surface cracks up to 40 mm long and through edge cracks several millimeters wide were seen in the PAM-Ti-6Al-4V plate (Fig. 8a), while the PAM-Ti-6Al-4V-0.1B plate is crack free (Fig. 8b). The ISM material was also rolled to plate without surface or edge cracks (Fig. 8c). Both boron-containing materials were subsequently rolled successfully to sheet. The ability to roll the as-cast material directly could therefore be attributed to the fine grain structure produced by trace boron addition. Extensive cracking observed in Ti-6Al-4V reconfirms that coarse as-cast microstructure has poor hot workability and grain refinement is essential before rolling into plates and sheets.

### 3.3 Tensile Properties of Ti-6Al-4V + 0.1B Plate and Sheet

The tensile properties of Ti-6Al-4V + 0.1B plates and sheets are summarized in Fig. 9 and Table 3. The mean  $\pm$  SD values for three tests conducted under each condition are listed. The variation in the measured yield and tensile strength among

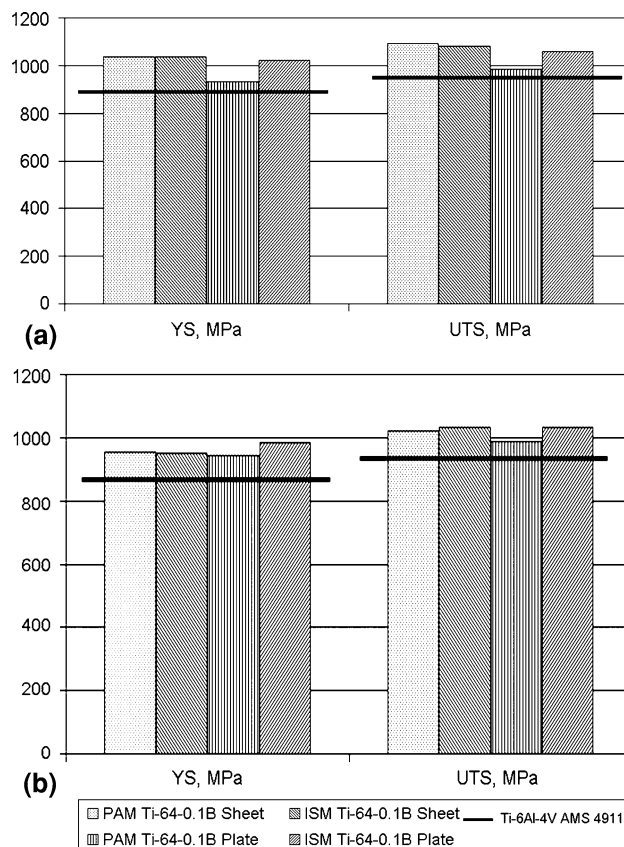


**Fig. 9** Yield strength (YS) and ultimate tensile strength (UTS) of plates and sheets of Ti-6Al-4V-0.1B in the transverse and rolling directions

the three samples is less than about 1% of the mean. The specifications for conventional Ti-6Al-4V plate and sheet (AMS 4911 S-basis) are used for comparison. The yield and ultimate strength of the plates and sheets in the rolling and transverse directions of the boron-containing alloys are approximately equal to the baseline values. The minor improvements

**Table 3 Tensile properties of rolled Ti-6Al-4V-0.1B (three tests per condition)**

Material	Condition ID	Test direction	YS, MPa	UTS, MPa	Elong. %
PAM Ti-64-0.1B sheet	PBS	Rolling	953 ± 5.9	1023 ± 4.2	14.6 ± 2.6
		Transverse	1038 ± 4.5	1094 ± 2.6	18.2 ± 1.0
ISM Ti-64-0.1B sheet	IBS	Rolling	950 ± 10.4	1033 ± 8.5	18.4 ± 2.9
		Transverse	1035 ± 3.6	1081 ± 5.1	15.9 ± 2.8
PAM Ti-64-0.1B plate	PBP	Rolling	945 ± 13.1	987 ± 11.5	13.5 ± 1.9
		Transverse	934 ± 4.0	983 ± 3.1	17.0 ± 0.2
ISM Ti-64-0.1B plate	IBP	Rolling	986 ± 2.1	1031 ± 0.6	14.6 ± 2.1
		Transverse	1021 ± 2.0	1060 ± 2.5	15.3 ± 3.1
Ti-6Al-4V		Rolling	861	930	10
AMS 4911		Transverse	903	951	10

The reported values are mean ± SD

**Fig. 10** Results of the double bend test samples from different sheet materials

in strength can be attributed to the small volume fraction of the strong TiB phase.

### 3.4 Formability of Sheets

The results of the double bend tests on sheets of the test materials are shown in Fig. 10. Two samples each of the boron-containing alloys were tested, while only one sample of the non-boron alloy was tested due to limited material availability. Sheets made from PAM-Ti-6Al-4V-0.1B were bent into the “Z” shape specified by ASTM E 290 without failure, while those made from ISM-Ti-6Al-4V-0.1B showed only partial success. Both these samples broke during the second bend. The non-boron PAM-Ti-6Al-4V failed on both bends. Due to a limited amount of material, additional tests to definitively establish a difference in formability between PAM-Ti-6Al-4V-0.1B and ISM-Ti-6Al-4V-0.1B were not carried out. Slightly higher amounts of interstitial impurity contents in ISM material are likely to cause reduced formability.

### 3.5 Microstructure of the Plates and Sheets

**3.5.1 Microstructure of Rolled Plates.** Figure 11 shows micrographs of the rolled PAM-Ti-6Al-4V-0.1B plate. It can be seen that the lamellar  $\alpha + \beta$  and TiB needles along prior- $\beta$  grain boundaries break up during rolling. Grain size reduction from 200 to 300  $\mu\text{m}$  (prior- $\beta$  grain size) in the as-cast material to about 20  $\mu\text{m}$  ( $\alpha$  grain size) after rolling can be observed. Globularization of the  $\alpha$  phase occurred after rolling in the

$\alpha + \beta$  phase field. Some of the TiB needles fragmented after rolling and the matrix flow filled the resulting gaps leaving no noticeable voids at low to moderate magnification. However, microvoids were observed near the tips of the TiB particles (Fig. 11c). These voids could be due to rolling at lower temperatures and unoptimized roll pass design.

The ISM-Ti-6Al-4V-0.1B ingot started out with a more equiaxed grain morphology (Fig. 5) compared with the columnar grain morphology of the PAM ingots (Fig. 4). Figure 12 shows microstructures of the ISM sample following a rolling reduction of 75%. As was seen in the PAM-Ti-6Al-4V-0.1B sample (Fig. 11), in the ISM samples the breakup of lamellar  $\alpha + \beta$  microstructure occurred and globularized during the rolling process with a small fraction of lamellar structures scattered throughout. Overall, the matrix filled in very well around the broken up needles. However, as with the PAM-Ti-6Al-4V-0.1B sample, microvoids are observed near the tips of the TiB needles (Fig. 12c). Compared to the PAM-Ti-6Al-4V-0.1B material, the ISM-Ti-6Al-4V-0.1B appears to be more globularized, probably the result of the finer initial microstructure in the ISM material.

The microstructure of the rolled plates of (non-boron) PAM-Ti-6Al-4V (Fig. 13) reinforces the observations in Fig. 8(a) regarding cracking of plates during rolling of the large grained material. The coarse columnar morphology in the as-cast condition and the associated strain incompatibility between the grains during rolling results in the formation of cracks and voids along grain boundaries.

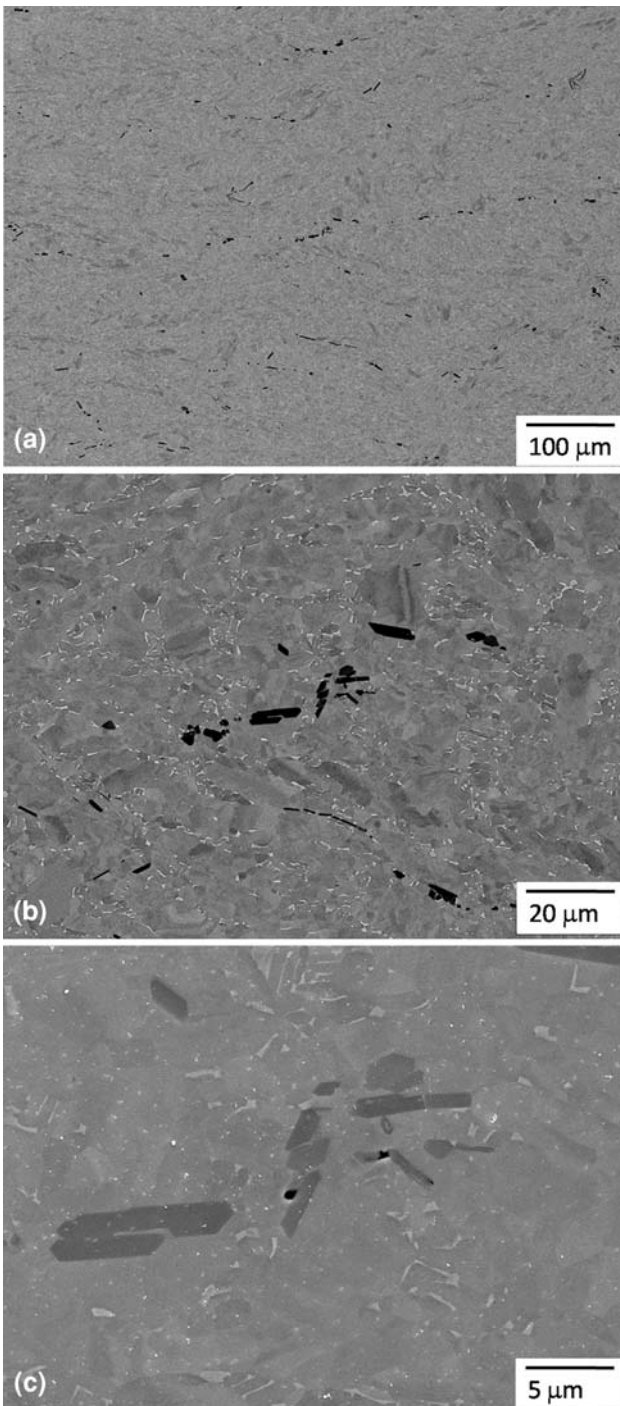


**Fig. 11** Micrograph of rolled plate of PAM Ti-6Al-4V-0.1B after 75% reduction: (a) low magnification (b) high magnification (c) voids at the end of TiB particles

**3.5.2 Microstructure of Rolled Sheets.** Figure 14 and 15 show micrographs of PAM-Ti-6Al-4V-0.1B and ISM-Ti-6Al-4V-0.1B sheets, respectively. The starting temperature for sheet rolling was 982 °C (1800 °F), or 28 °C (50 °F) higher than that used in rolling of the plates. Unlike the rolled plates, microvoids were not observed near the ends of the TiB needles. The increase in rolling temperature apparently allowed the matrix to flow more easily between the broken TiB needles and lower the temperature drop during rolling.

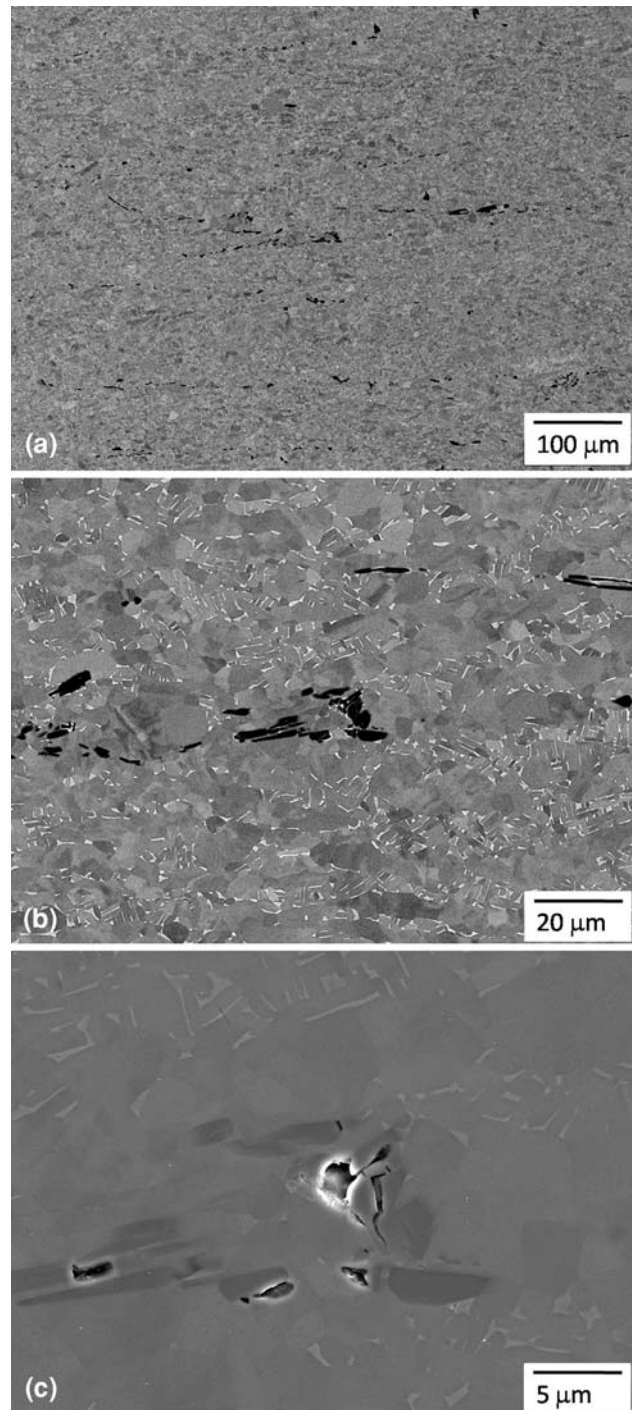


**Fig. 12** Micrograph of rolled plate of ISM Ti-6Al-4V-0.1B after 75% reduction: (a) low magnification (b) high magnification (c) voids at the ends of TiB particles

The extent of globularization in the rolled plate and the heat-treated sheet material for the PAM-Ti-6Al-4 V-0.1B sample (Fig. 11, 14) appear to be about the same, but the overall grain size has been reduced from about 20 μm in the plate to 5-10 μm in the sheet due to the additional deformation. This grain size is comparable to the conventionally processed Ti-6Al-4V sheet although the amount of deformation introduced is typically much higher than that usually introduced in these sheets. Another noticeable feature in the microstructures

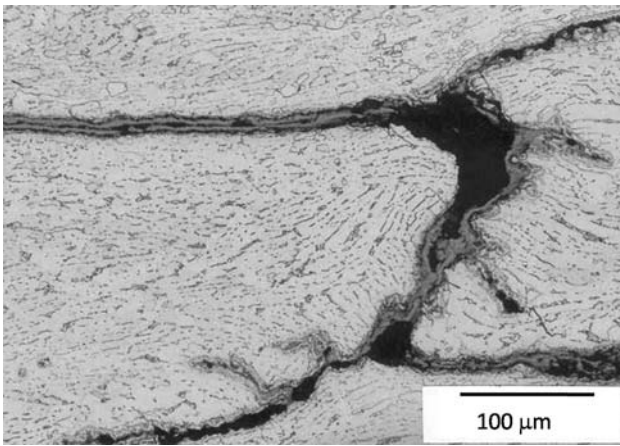


**Fig. 13** Micrograph of the rolled plate of PAM-Ti-6Al-4V

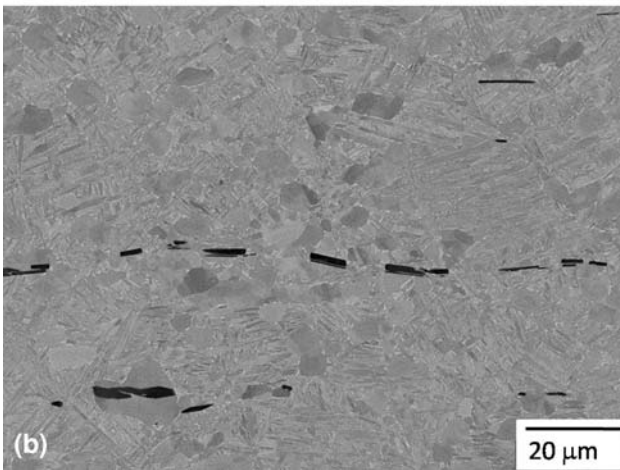
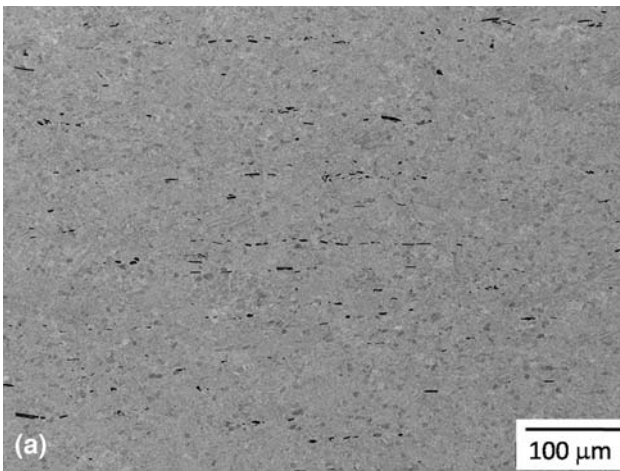


**Fig. 14** Micrograph of rolled sheet of PAM-Ti-6Al-4V-0.1B after 92% reduction from the cast state: (a) low magnification (b) high magnification. The rolling direction is horizontal

shown in Fig. 14(a) and 15(a) is that TiB particles are distributed throughout the matrix, and are aligned in the rolling direction. Figure 16 shows that after stress relief heat treatment at 788 °C for 15 min, the microstructure of ISM-Ti-6Al-4V-0.1B sheet does not change significantly from the as-rolled condition, which is as expected.

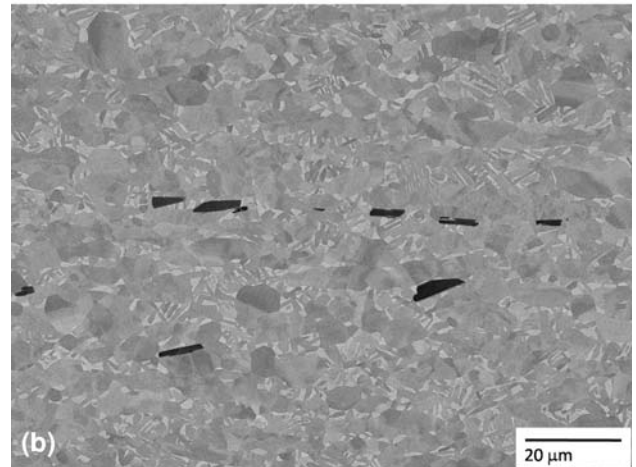
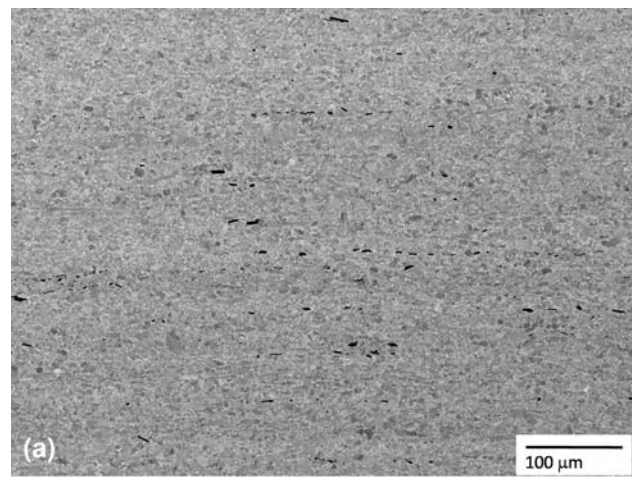


**Fig. 15** Micrograph of rolled sheet of ISM-Ti-6Al-4V-0.1B after 92% reduction, without heat treatment (a) low magnification (b) high magnification. The rolling direction is horizontal

#### 4. Summary and Conclusions

The addition of 0.1% boron to Ti-6Al-4V reduces as-cast grain size by an order of magnitude to about 200 μm. The reduction in grain size is observed in ingots prepared by both plasma arc melting (PAM) and induction skull melting (ISM) techniques. The reduction in grain size enables direct rolling of cast Ti-6Al-4V-0.1B ingots at billet temperatures ranging from 954 to 982 °C (1750-1800 °F), which are used in the rolling of conventionally produced Ti-6Al-4V blooms. Rolling of cast Ti-6Al-4V under similar conditions lead to extensive cracking due to coarse starting grain size.

Trace boron additions result in the formation of TiB along prior-β grain boundaries. The TiB phase appears as needles, which are randomly oriented. Hot rolling of the cast ingots results in a fragmentation of the TiB needles. At a sufficiently high temperature (~980 °C), the relatively soft metallic titanium matrix is able to flow plastically and fill up any microvoids that may form between the fragments. As a result of the imposed deformation, the TiB particles tend to align the rolling direction. The tensile yield strength, ultimate strength, and ductility of rolled plates and sheets of Ti-6Al-4V-0.1B are comparable to the properties of conventionally produced Ti-6Al-4V (AMS 4911).



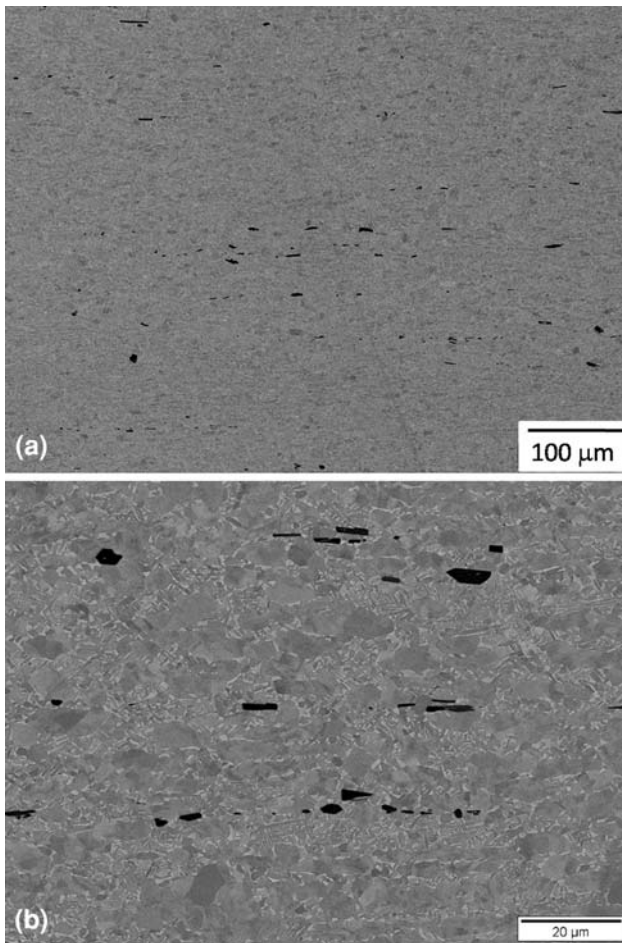


**Fig. 16** Micrograph of rolled sheet of ISM-Ti-6Al-4V-0.1B after 92% reduction, after heat treatment at 788 °C for 15 min (a) low magnification (b) high magnification. The rolling direction is horizontal

In summary, microalloying with 0.1 wt.% or 1000 parts per million of boron improves the processability of the cast ingots and enables direct rolling of the cast ingots. Therefore, by eliminating the ingot breakdown step, there is a potential for decreasing the overall time and cost of producing titanium parts.

### Acknowledgments

This work was partially funded by the Edison Materials Technology Center (EMTEC), Kettering, Ohio, through Core Technology Project CT-86.

### References

1. M.J. Donachie Jr., *Titanium: A Technical Guide*, ASM International, Metals Park, OH, 1988
2. S.L. Semiatin, V. Seetharaman, and I. Weiss, The Thermomechanical Processing of Alpha/Beta Titanium Alloys, *JOM*, 1997, **49**, p 33–39
3. S.L. Semiatin, V. Seetharaman, and I. Weiss, Hot Working of Titanium Alloys—An Overview, *Advances in the Science and Technology of Titanium Alloy Processing*, I. Weiss, R. Srinivasan, D. Eylon, P. Bania, and S.L. Semiatin, Eds., TMS, Warrendale, PA, ISBN 0-87339-324-4, 1997, p 3–73
4. S. Tamirisakandala, R.B. Bhat, J.S. Tiley, and D.B. Miracle, Grain Refinement of Cast Titanium Alloys via Trace Boron Addition, *Scripta Mater.*, 2005, **53**, p 1421–1426
5. I. Sen, S. Tamirisakandala, D.B. Miracle, and U. Ramamurty, Microstructural Effects on the Mechanical Behavior, of B-modified Ti-6Al-4V Alloys, *Acta Mater.*, 2007, **55**, p 4983–4993
6. J. Zhu, A. Kamiya, T. Yamada, W. Shi, and K. Naganuma, *Mater. Sci. Eng. A*, 2003, **339**, p 53–62
7. H.T. Tsang, C.G. Chao, and C.Y. Ma, Effects of Volume Fraction of Reinforcement on Tensile and Creep Properties of In-Situ TiB/Ti MMC, *Scripta Mater.*, 1997, **37**, p 1359–1365
8. S. Gorsse, Y. Le Petitcorps, S. Matar, and F. Rebillat, Investigation of the Young's Modulus of TiB Needles In Situ Produced in Titanium Matrix Composite, *Mater. Sci. Eng. A*, 2003, **340**, p 80–87
9. L. Wang, M. Niinomi, S. Takahashi, M. Hagiwara, S. Emura, Y. Kawabei, and S.-J. Kim, Relationship Between Fracture Toughness and Microstructure of Ti-6Al-2Sn-4Zr-2Mo Alloy Reinforced with TiB Particles, *Mater. Sci. Eng. A*, 1999, **263**, p 319–325
10. C. Schuh and D.C. Dunand, Load Transfer During Transformation Superplasticity of Ti-6Al-4V/TiB Whisker-reinforced Composites, *Scripta Mater.*, 2001, **45**, p 631–638
11. S. Gorsse and D.B. Miracle, Mechanical Properties of Ti-6Al-4V/TiB Composites with Randomly Oriented and Aligned TiB Reinforcements, *Acta Mater.*, 2003, **51**, p 2427–2442
12. S. Ranganath, M. Vijayakumar, and J. Subramanyam, Combustion-assisted Synthesis of Ti-TiB-TiC Composite via the Casting Route, *Mater. Sci. Eng. A*, 1992, **149**, p 253
13. C.F. Yolton and J.H. Moll, Evaluation of a Discontinuously Reinforced Ti-6Al-4V Composite, *Titanium '95: Science and Technology*, Vol. 3, P.A. Blenkinsop, W.J. Evans and H.M. Flower, Eds., The Institute of Materials, London, 1996, p 2755
14. Z. Fan, H.J. Niu, A.P. Miodownik, T. Saito, and B. Cantor, Microstructure and Mechanical Properties of In Situ Ti/TiB MMCs Produced by the Blended Elemental Powder Metallurgy Method, *Key Engineering Materials*, Vol. 127-131, Trans Tech. Publications, Switzerland, 1997, p 423
15. T. Yamaguchi, H. Morishita, S. Iwase, S. Yamada, T. Furuta, and T. Saito, "Development of P/M Titanium Engine Valves," *SAE 2000 World Congress*, Detroit, MI, March 6-9, 2000, SAE Technical Paper 2000-01-0905, SAE International, Warrendale, PA
16. S. Abkowitz and P. Wehrauch, Trimming the Cost of MMCs, *Adv. Mater. Process.*, 1989, **136**(1), p 31
17. S. Abkowitz, P. Wehrauch, H. Heussi, and S. Abkowitz, P/M Titanium Matrix Composites: From War Games to Fun and Games, *Titanium '95: Science and Technology*, Vol. 3, P.A. Blenkinsop, W.J. Evans and H.M. Flower, Eds., The Institute of Materials, London, 1996, p 2722
18. R. Srinivasan, D. Miracle, and S. Tamirisakandala, Direct Rolling of As-Cast Ti-6Al-4V Modified with Trace Additions of Boron, *Mater. Sci. Eng. A*, 2008, **487**, p 541–551
19. D.B. Miracle, R.B. Bhat, S. Tamirisakandala, and J.S. Tiley, "Titanium Alloy Microstructural Refinement Method and High Temperature, High Strain Rate Superplastic Forming of Titanium Alloys," International Patent S.No. 60/528,660 filed Dec. 11, 2003